Performance analysis of active noise control over a spatial region

Jihui (Aimee) Zhang*§, Thushara D. Abhayapala*, Naoki Murata†, Prasanga N. Samarasinghe*, Yu Maeno, and Yuki Mitsufuji†‡
* Audio & Acoustic Signal Processing Group, The Australian National University, Canberra, Australia
† Sony AI, Tokyo, Japan, ‡ Sony Group Corporation, Tokyo, Japan
§ School of Electrical Engineering and Computer Science, The University of Queensland, Brisbane, Australia

***Abstract*—Active noise control (ANC) over region(s), or spatial ANC, extends the noise control from one or more points to the entire region(s). This paper proposes an evaluation method to predict the 'noise reduction performance over the entire region' (NRR) for any given spatial ANC system. This method formulates the acoustic potential energy of the residual signals over the region into spherical/cylindrical-harmonics coefficients (also named as 'wave-domain coefficients'), and further decomposes it into three components related to the coherence between reference signals at the reference microphones and primary signals over the region, filter coefficients, and an uncontrollable term due to physical and practical constraints. This analytical tool provides insight into the contribution of each component to the overall noise reduction performance over the entire region.**

I. Introduction

Active noise control (ANC) over a spatially extended region, which is termed as 'Spatial ANC', is a challenging task as the aim is to create a large quiet zone for multiple listeners in a sizable space [1]. Spatial ANC systems are equipped with multiple sensors and multiple secondary sources. For practical scenarios with constraints on numbers and locations of sensors and secondary sources, it is important to investigate the maximum achievable noise reduction performance before implementing the ANC system. For applications targeting the noise control over a region [2]–[6], it is critical to evaluate the performance over the entire region directly.

In the literature, Kuo investigated the relation between the minimum residual signal and the coherence between signals at the reference microphone and the error microphone for single channel ANC system [7]. In our previous work [8], we provided a theoretical analysis of the fundamental limitation of the noise reduction performance of the multichannel ANC system and investigated the contributions of each component in the energy of residual signals, which only focused on the evaluation on the error microphone points. For evaluating the noise reduction performance over the entire region (NRR), Chen et al. investigated NRR through noise pattern analysis of the primary noise field [9], [10] and Zhang et al. [11], [12] investigated NRR through subspace analysis of the secondary paths of the ANC systems. However, these works haven't considered the relation between NRR and the coherence between reference signals at the reference microphones and error signals over the region, and the relation between NRR and the filters in different minimization methods. To the best of our knowledge, a theoretical analysis of the fundamental limitation of NRR and the contribution of each component in the energy of residual signals over the region have not been conducted yet.

In this paper, we focus on the evaluation over the region directly, and theoretically evaluate NRR for any given spatial ANC system before implementing the ANC system. We formulate the total acoustic potential energy (APE) of the residual signals over the region into spherical/cylindrical-harmonics coefficients, and decompose it into components related to signal coherence over the region, filter, and the non-controllable terms due to the physical setup of the ANC systems. In the numerical simulations, we show the evaluation examples for given spatial ANC systems using the proposed method under different setups and different minimization methods.

The rest of the paper is organized as follows: Section II presents the problem formulation, and Section III decomposes the APE of residual signal over the entire region in terms of different components. Section IV presents simulation results of using the proposed method to evaluate noise reduction performance over the entire region of interest, and Section V draws some conclusions and future works.

II. Problem Formulation

A. Spatial active noise control system

Consider a spatial feedforward ANC system with Q error microphones, P reference microphones and L secondary

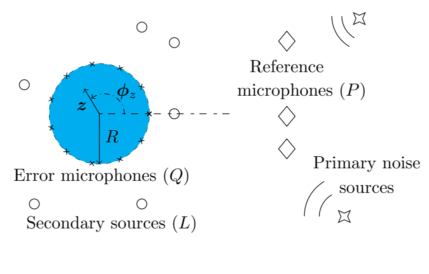

Figure 1. Spatial ANC systems, with P reference microphones $\diamond$, primary noise sources $\star$, Q error microphones $\times$, and L secondary loudspeakers $\circ$.

[0]Correspondence: jihuiaimee.zhang@uq.edu.au

sources (loudspeakers), as shown in Fig.1. The region of interest is a circular/spherical region with a radius R. We assume that the noise sources are located outside the region of interest, and the error microphones are located on the boundary of the region.

The residual signal at any arbitrary point $\boldsymbol{z}$ inside the region is given by

$$e(\boldsymbol{z}, k) = \nu(\boldsymbol{z}, k) + s(\boldsymbol{z}, k), \tag{1}$$

where $k = 2\pi f/c$ is the wavenumber, f is the frequency, c is the speed of sound propagation, $\nu(\boldsymbol{z}, k)$ and $s(\boldsymbol{z}, k)$ are the primary sound field and the secondary sound field at the point $\boldsymbol{z}$, respectively.

The spherical/cylindrical-harmonics based wave equation solution can decompose any incident wave field observed in a region into spherical/cylindrical-harmonics basis functions [13]. In this paper, we use the cylindrical-harmonics decomposition in two dimensional space as an example.

The primary sound field $v(\boldsymbol{z}, k)$ observed at any arbitrary point $\boldsymbol{z}$ inside the region can be decomposed into

$$v(\boldsymbol{z}, k) = \sum_{m=-\infty}^{\infty} \beta_m(k) J_m(kr) \exp(im\phi_{\boldsymbol{z}}), \tag{2}$$

where $J_m(\cdot)$ is the Bessel function of order m and $\exp(\cdot)$ denotes the exponential function [13]. The decomposition coefficients $\beta_m(k)$ represent the primary noise field in the cylindrical-harmonics domain (also named as 'wave domain'). Within the circular region $r \le R$, we can use a finite number of modes to approximate the noise field [14], thus (2) reduces to

$$v(\boldsymbol{z}, k) \approx \sum_{m=-M}^{M} \beta_m(k) J_m(kr) \exp(im\phi_{\boldsymbol{z}}), \tag{3}$$

where $M = \lceil ekR/2 \rceil$ [14].

Similarly, the generated secondary sound field inside the control region can also be represented by

$$s(\boldsymbol{z}, k) \approx \sum_{m=-M}^{M} \gamma_m(k) J_m(kr) \exp(im\phi_{\boldsymbol{z}}), \tag{4}$$

where coefficients $\gamma_m(k)$ represent the secondary sound field in the wave domain.

Substituting (3) and (4) into (1), the residual signals can be represented by

$$e(\boldsymbol{z}, k) \approx \sum_{m=-M}^{M} \underbrace{(\beta_m(k) + \gamma_m(k))}_{\alpha_m(k)} J_m(kr) \exp(im\phi_{\boldsymbol{z}}), \tag{5}$$

where $\alpha_m(k)$ is the residual signal decomposition coefficients.

APE of the residual signals over the entire region $\varepsilon(k)$ can be represented as [2]

$$\varepsilon(k) \simeq E\left\{\boldsymbol{\alpha}^H(k)\boldsymbol{O}(k)\boldsymbol{\alpha}(k)\right\}, \tag{6}$$

where $\boldsymbol{O}(k) = \mathrm{diag}(\cdots, o_m(k), \cdots)$ is a diagonal matrix of APE weights, $E\{\cdot\}$ is the expectation operator, and $\boldsymbol{\alpha}(k) = [\alpha_{-M}, \cdots, \alpha_m, \cdots, \alpha_M]^T$ is the wave-domain coefficients of the residual signals over the region [15]. Within a circular region with a radius of R, the number of modes to represent the entire region is $2M + 1$. The APE weights are given by $o_m(k) = 2\pi \int_0^R (J_m(kr))^2 r dr, m \in [-M, M]$ [2].

When the ANC is on, the error signals at error microphone points can be directly measured. We can estimate the wave domain coefficients $\alpha_m(k)$ from (5), and further estimate APE of the residual signals over the entire region from (6), which is a good indicator of the instantaneous energy of the residual sound field over the entire region. However, in this paper, to evaluate the noise reduction performance before implementing the ANC system, we do not have access to $e(\boldsymbol{z}, k)$ or $\alpha_m(k)$. In the following sections, we will formulate APE over the region as other measurable quantities for a given spatial ANC setup.

B. Acoustic potential energy over the region

In this subsection, we formulate the APE of the residual signals over the entire region $\varepsilon(k)$, and represent it in terms of the wave-domain coefficients of the residual signals over the region [2].

In matrix form, for feed-forward ANC system, the wave-domain coefficients of the residual signals $\boldsymbol{\alpha}(k)$ can be also represented as

$$\boldsymbol{\alpha}(k) = \boldsymbol{\beta}(k) + \boldsymbol{\gamma}(k) = \boldsymbol{\beta}(k) + \boldsymbol{\eta}(k)\boldsymbol{W}(k)\boldsymbol{x}(k), \tag{7}$$

where $\boldsymbol{\beta}(k) = [\beta_{-M}, \cdots, \beta_m, \cdots, \beta_M]^T$ and $\boldsymbol{\gamma}(k) = [\gamma_{-M}, \cdots, \gamma_m, \cdots, \gamma_M]^T$. $\boldsymbol{\eta}(k)$ is a $(2M + 1) \times L$ matrix of the wave-domain transfer functions between loudspeakers and the region, and its estimation $\hat{\boldsymbol{\eta}}(k)$ is assumed to be prior knowledge. $\boldsymbol{W}(k)$ is a $L \times P$ matrix of filters, and $\boldsymbol{x}(k) = [x_1(k), \cdots, x_P(k)]^T$ denotes the reference signals. Here onward, the frequency dependent k is omitted for notational simplicity.

Substituting (7) into (6), APE of residual signals over the region can be rewritten as

$$\begin{aligned}\varepsilon \simeq E\{&\boldsymbol{\beta}^H\boldsymbol{O}\boldsymbol{\beta} + \boldsymbol{\beta}^H\boldsymbol{O}\boldsymbol{\eta}\boldsymbol{W}\boldsymbol{x} + \boldsymbol{x}^H\boldsymbol{W}^H\boldsymbol{\eta}^H\boldsymbol{O}\boldsymbol{\beta} \\ &+ \boldsymbol{x}^H\boldsymbol{W}^H\boldsymbol{\eta}^H\boldsymbol{O}\boldsymbol{\eta}\boldsymbol{W}\boldsymbol{x}\}.\end{aligned} \tag{8}$$

In the following section, we seek to further analyze APE of residual signals over the region ε in (8) by investigating the different factors that can influence ε.

III. Analysis of Potential Energy of Residual Signals over the Region

We define the weighted coefficients of primary signals and the estimated secondary path over the region as $\tilde{\boldsymbol{\beta}} \triangleq \boldsymbol{O}^{1/2}\boldsymbol{\beta}$ and $\tilde{\boldsymbol{\eta}} \triangleq \boldsymbol{O}^{1/2}\hat{\boldsymbol{\eta}}$, respectively. Equation (8) can be estimated as

$$\begin{aligned}\varepsilon \simeq\ & E\left\{\tilde{\boldsymbol{\beta}}^H\tilde{\boldsymbol{\beta}}\right\} + E\left\{\tilde{\boldsymbol{\beta}}^H\tilde{\boldsymbol{\eta}}\boldsymbol{W}\boldsymbol{x}\right\} + E\left\{\boldsymbol{x}^H\boldsymbol{W}^H\tilde{\boldsymbol{\eta}}^H\tilde{\boldsymbol{\beta}}\right\} \\ &+ E\left\{\boldsymbol{x}^H\boldsymbol{W}^H\tilde{\boldsymbol{\eta}}^H\tilde{\boldsymbol{\eta}}\boldsymbol{W}\boldsymbol{x}\right\}.\end{aligned} \tag{9}$$

In this section, we analyze the vector space over the region generated by the ANC system, and discuss components contributed to APE of residual signals over the region in (9).

A. System space over the region and primary noise projection

Each column of $\tilde{\boldsymbol{\eta}}$ are not necessarily independent of each other. To reveal its underlying structure, we express $\tilde{\boldsymbol{\eta}}$ in terms of its singular value decomposition (SVD) form as

$$\tilde{\boldsymbol{\eta}} = \boldsymbol{A}\boldsymbol{\Sigma}\boldsymbol{B}^H, \tag{10}$$

where $(2M+1) \times (2M+1)$ matrix $\boldsymbol{A} = [\boldsymbol{a}_1, \cdots, \boldsymbol{a}_{2M+1}]$ contains left-singular vectors, $L \times L$ matrix $\boldsymbol{B} = [\boldsymbol{b}_1, \cdots, \boldsymbol{b}_L]$ contains right-singular vectors, and $(2M+1) \times L$ rectangular diagonal matrix $\boldsymbol{\Sigma}$ contains singular values. The non-zero diagonal entries of $\boldsymbol{\Sigma}$ are denoted by σ_d, $d = 1, \cdots, D$, where $D = \text{rank}(\tilde{\boldsymbol{\eta}}) \leqslant \min\{2M+1, L\}$. Also note that, by the definition of SVD, $\boldsymbol{A}\boldsymbol{A}^H = \boldsymbol{I}_M$ and $\boldsymbol{B}\boldsymbol{B}^H = \boldsymbol{I}_L$, where $\boldsymbol{I}_M$ and $\boldsymbol{I}_L$ are identity matrices. $\acute{\boldsymbol{A}} = [\boldsymbol{a}_1, \cdots, \boldsymbol{a}_D]$ represents the vector space over the region generated by the ANC system and $\grave{\boldsymbol{A}} = [\boldsymbol{a}_{D+1}, \cdots, \boldsymbol{a}_{2M+1}]$ represents the system null space.

To project the primary noise into the system space, we rewrite $\tilde{\boldsymbol{\beta}}$ as

$$\tilde{\boldsymbol{\beta}} = \boldsymbol{A}\boldsymbol{y}, \tag{11}$$

where $\boldsymbol{y} = [y_1, \cdots, y_{2M+1}]^T = \boldsymbol{A}^H\tilde{\boldsymbol{\beta}}$. It also can be decomposed into two components

$$\tilde{\boldsymbol{\beta}} = \acute{\boldsymbol{\beta}} + \grave{\boldsymbol{\beta}} : \tag{12}$$

The first component is the primary noise which can be projected to the system space ($\acute{\boldsymbol{\beta}} = \acute{\boldsymbol{A}}\acute{\boldsymbol{y}}$) where $\acute{\boldsymbol{y}} = [y_1, \cdots, y_D]^T$, and the second component is the primary noise which can be projected to the system null space ($\grave{\boldsymbol{\beta}} = \grave{\boldsymbol{A}}\grave{\boldsymbol{y}}$), where $\grave{\boldsymbol{y}} = [y_{D+1}, \cdots, y_{2M+1}]^T$.

B. Components contributed to APE of residual signals

Taking the eigen analysis of the reference signals $\boldsymbol{x}$, the power spectral density matrix of the reference signals is a Hermitian matrix, which can be decomposed by

$$E\{\boldsymbol{x}\boldsymbol{x}^H\} = \boldsymbol{U}\boldsymbol{\Lambda}\boldsymbol{U}^{-1} = \boldsymbol{U}\boldsymbol{\Lambda}\boldsymbol{U}^H, \tag{13}$$

where $\boldsymbol{U}$ is the $P \times P$ eigen-vector matrix and $\boldsymbol{\Lambda}$ is a $P \times P$ diagonal matrix with eigen values. We denote λ_n as the n^{th} non-zero eigen value, $n = 1, \cdots, N$, where $N \leqslant P$.

Since eigenvectors $\boldsymbol{u}_n$ corresponding to distinct eigenvalues are orthogonal, the reference signals $\boldsymbol{x}$ can be represented into

$$\boldsymbol{x} = \sum_{n=1}^{N} \chi_n \boldsymbol{u}_n = \tilde{\boldsymbol{U}}\boldsymbol{\chi}, \tag{14}$$

where $\tilde{\boldsymbol{U}} = [\boldsymbol{u}_1, \cdots, \boldsymbol{u}_N]$ are the eigen vectors corresponding to the non-zero eigen values in $\boldsymbol{\Lambda}$, and the components of $\boldsymbol{\chi} = \tilde{\boldsymbol{U}}^H\boldsymbol{x}$ are statistically independent.

Substituting (11), (10) and (14) into (9), (9) can be rewritten as

$$\varepsilon \simeq E\{\boldsymbol{y}^H\boldsymbol{y}\} + E\{\boldsymbol{y}^H\boldsymbol{\Sigma}\tilde{\boldsymbol{W}}\boldsymbol{\chi}\} + E\{\boldsymbol{\chi}^H\tilde{\boldsymbol{W}}^H\boldsymbol{\Sigma}^H\boldsymbol{y}\} + E\{\boldsymbol{\chi}^H\tilde{\boldsymbol{W}}^H\boldsymbol{\Sigma}^H\boldsymbol{\Sigma}\tilde{\boldsymbol{W}}\boldsymbol{\chi}\}, \tag{15}$$

where $L \times N$ matrix $\tilde{\boldsymbol{W}} = \boldsymbol{B}^H\boldsymbol{W}\tilde{\boldsymbol{U}}$ represents the transformed filter. Let $\tilde{w}_{\ell n}$ is the $(\ell, n)^{\text{th}}$ element of $\tilde{\boldsymbol{W}}$, then we define the vector $\tilde{\boldsymbol{w}}_\ell \triangleq [\tilde{w}_{\ell 1}, \cdots, \tilde{w}_{\ell N}]$.

Theorem 1: For a given spatial ANC system, since both the correlation matrix between the primary signal coefficients and the reference signals $E\{\boldsymbol{\beta}\boldsymbol{x}^H\}$ and the power spectral density matrix of the primary signal coefficients $E\{\boldsymbol{\beta}\boldsymbol{\beta}^H\}$ can be pre-measured, the potential energy of residual signals over the region (15) can be decomposed by a sum over each eigen channel of the weighted secondary path coefficients as

$$\begin{aligned}\mathcal{E} \simeq &\sum_{i=1}^{D} \big(1 - \sum_{n=1}^{N} C_{y_i\chi_n}\big) E\{y_i y_i^H\} + \\ &\sum_{i=1}^{D} |\sigma_i|^2 \Big[\big(\tilde{\boldsymbol{w}}_i + \frac{E\{y_i\boldsymbol{\chi}^H\}}{\sigma_i}\tilde{\boldsymbol{\Lambda}}^{-1}\big)\tilde{\boldsymbol{\Lambda}}\big(\tilde{\boldsymbol{w}}_i + \frac{E\{y_i\boldsymbol{\chi}^H\}}{\sigma_i}\tilde{\boldsymbol{\Lambda}}^{-1}\big)^H\Big] \\ &+ \sum_{i=D+1}^{2M+1} E\{y_i y_i^H\}\end{aligned} \tag{16}$$

where $\tilde{\boldsymbol{\Lambda}}$ is a $N \times N$ diagonal matrix whose diagonal elements are the non-zero diagonal elements of $\boldsymbol{\Lambda}$, $E\{y_i\boldsymbol{\chi}^H\} = \boldsymbol{a}_i^H\boldsymbol{O}^{1/2}E\{\boldsymbol{\beta}\boldsymbol{x}^H\}\tilde{\boldsymbol{U}}$, $E\{y_i y_i^H\} = \boldsymbol{a}_i^H\boldsymbol{O}^{1/2}E\{\boldsymbol{\beta}\boldsymbol{\beta}^H\}\boldsymbol{O}^{1/2}\boldsymbol{a}_i$, σ_i is the ith non-singular value of the weighted secondary path coefficients matrix. $C_{y_i\chi_n}$ is the coherence between the transformed primary signal coefficients y_i and the eigen component of the reference signal χ_n,

$$C_{y_i\chi_n} \triangleq \frac{|E\{y_i\chi_n^H\}|^2}{E\{y_i y_i^H\}E\{\chi_n\chi_n^H\}} = \frac{\|\boldsymbol{a}_i^H\boldsymbol{O}^{\frac{1}{2}}E\{\boldsymbol{\beta}\boldsymbol{x}^H\}\boldsymbol{u}_n\|^2}{\boldsymbol{a}_i^H\boldsymbol{O}^{\frac{1}{2}}E\{\boldsymbol{\beta}\boldsymbol{\beta}^H\}\boldsymbol{O}^{\frac{1}{2}}\boldsymbol{a}_i\lambda_n}. \tag{17}$$

Here, $\boldsymbol{a}_i$, σ_i, $\boldsymbol{O}$, $\boldsymbol{u}_n$, λ_n all depend on the given system setup, given noise source position, and given noise signals.

The proof is given in the Appendix A. We have the following comments:

1) Component related to signal coherence over the region: The first summation term in (16) $\mathcal{E}_1$ depends on the coherence between the transformed primary signal coefficients y_i and the transformed reference signals χ_n, and the power spectral density of the transformed primary signal coefficients $E\{y_i y_i^H\}$.

2) Component related to the filter: The second summation term in (16) $\mathcal{E}_2$ depends on the transformed filter $\tilde{\boldsymbol{W}}$, which is the filter applied in the ANC algorithm projected onto the system space ($\acute{\boldsymbol{\beta}}$). Here, we also provide a method to calculate the optimal filter over the region, which minimizes the APE of the residual signals over the entire region. If we set $\mathcal{E}_2$ to zero, filter $\tilde{\boldsymbol{W}}$ is optimized. We can then obtain the corresponding optimal filter $\boldsymbol{W}^o$.

3) Component related to the system null space: The third summation term in (16) $\mathcal{E}_3$ is due to the energy of the primary signals at the region of interest projected onto the null space of the system ($\grave{\boldsymbol{\beta}}$). This represents the noise field which cannot be controlled as it is in the null space. This also indicates the limitation of a given spatial ANC system.

IV. Simulation

A. Simulation setup

We conduct the simulations in a 2D reverberant environment, which is modeled as a cuboid room with dimension

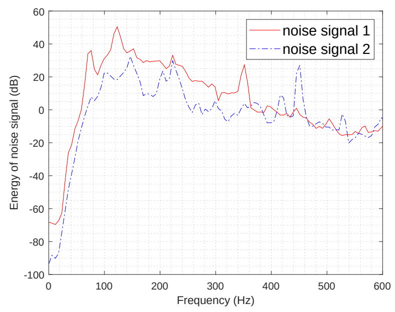

Figure 2. (Color online) Frequency spectrum of the noise signals.

of [6, 6] m and simulated by the image source method [16], [17] with the image order of 10. The reflection coefficients are set to [0.95, 0.9, 0.8, 0.7]. We assume a primary noise field generated by two point sources, which are outside of the secondary source array and emit uncorrelated noise signals (Fig. 2). We evaluate spatial ANC performance over $[100-500]$ Hz as the two noise signals are dominant in this frequency range.

We conduct ANC in two different cases, as shown in Fig. 3. For the circular region of interest with a radius of 0.4 m, $2M+1=11$ error microphones have been equiangularly placed on the boundary. Four reference microphones and a circular secondary source array have been placed outside the region. White Gaussian noise with signal-to-noise ratio of 40 dB is added to each microphone recording to simulate the internal thermal noise.

We evaluate APE reduction over the entire region (APER) and the contribution of each component (CO_1, CO_2, CO_3). The APE reduction over the region can be represented by APER $= -10\log_{10}[\mathcal{E}/E\{\boldsymbol{\nu}^H\boldsymbol{O}\boldsymbol{\nu}\}]$, where $E\{\boldsymbol{\nu}^H\boldsymbol{O}\boldsymbol{\nu}\}$ denotes the APE of the primary noise field over the region. The contribution of the j^{th} component is $CO_j = -10\log_{10}[\mathcal{E}_j/\mathcal{E}]$, where $\mathcal{E}_j, j=1,2,3$ is each component in (16). Spatial ANC algorithms mainly solve three different minimization problems: 1) minimize the residual signals over error microphone points [18] (**Points**), 2) minimize APE of the error signal over the region [2] (**RegionAPE**), and 3) minimize wave-domain coefficients over the region [19] (**Coef**). CO_1 and CO_3 are not affected by the minimization method, while CO_2 differs from different minimization methods. Here, in this paper, we use the optimal solution in each minimization method. Any adaptive filter $\boldsymbol{W}$ can be applied to evaluate a specific adaptive algorithm.

B. Simulation results

The APER results are shown in Fig. 4. For a given system setup, the higher the value of APER, the more noise reduction can be achieved over the entire region. In case 1, the number of loudspeakers is only enough to control the noise field over the region up to 300 Hz, but it is not enough to control the noise field beyond 300 Hz. Therefore, in [100, 300] Hz, all three methods result in same APER; in [300, 500] Hz,

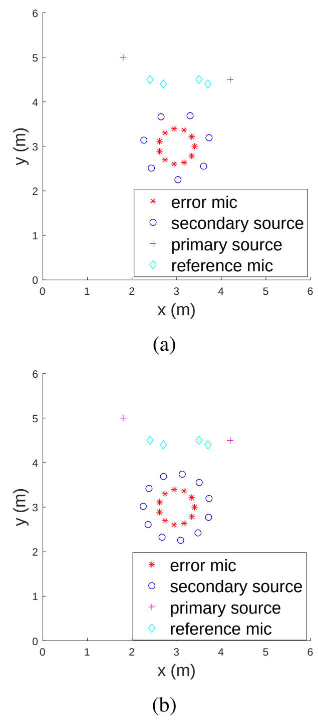

Figure 3. Spatial ANC systems with four reference microphones ◇, two primary sources +, eleven error microphones ∗, and (a) seven loudspeakers ∘ in case 1; (b) 11 loudspeakers ∘ in case 2.

RegionAPE achieves the highest APER and **Coef** achieves the lowest APER. In case 2, as the number of loudspeakers is enough to control the noise field over the entire evaluation frequency range, all three methods result in the same APER. In [100, 300] Hz, the APER performance is the same as in case 1; in [300, 500] Hz, APER performance is better than in case 1.

The contributions of each component are shown in Fig. 5. For a given system setup, the lower the value of CO_j, the more the corresponding contribution to APE of residual signals.

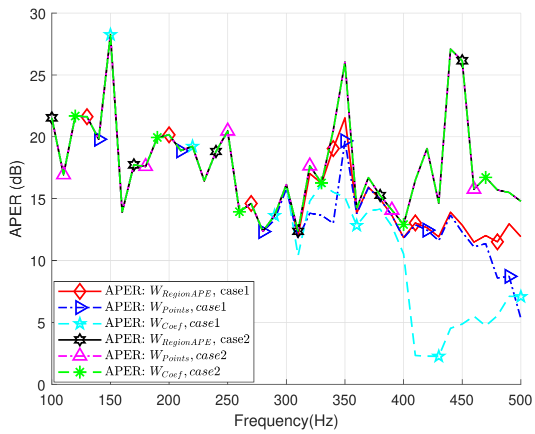

Figure 4. APER in both cases.

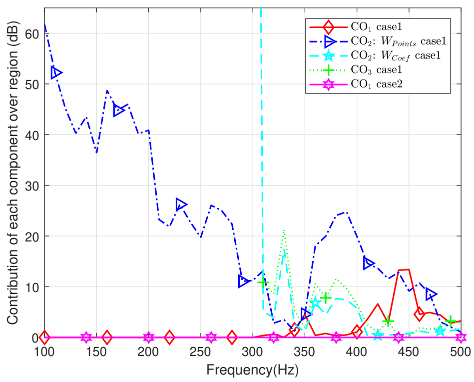

Figure 5. Contribution of each component in both cases.

In case 1, within the range of [100, 300] Hz, for all three minimization methods, CO_1 makes the dominant contribution, and CO_3 is zero due to the projection onto the null space being zero; within the range of [300, 500] Hz, all CO_1, CO_2 and CO_3 make significant contributions. In case 2, as the number of loudspeakers is enough to control the noise field over entire region, there is no contribution from CO_3, and CO_1 makes the dominant contribution to $\mathcal{E}$.

V. Conclusion

In this work, we proposed an evaluation method to predict the potential energy reduction over the entire region of interest before the ANC systems are implemented. Considering the coherence between reference signals and error coefficients over the region, for any given spatial ANC setup and minimization method, this method can provide more insight into the different contributions of each factor due to the effect of coherence, filter, and uncontrollable null space. The simulation results validate the effectiveness of this evaluation method. In this work, we assume a circular or spherical error microphone array, so that the wave-domain coefficients can be captured accurately, which might not be possible in some applications. Incorporating the extra error due to the measurement inaccuracy of wave-domain coefficients and the remaining error due to the degree of non-causality [20] in the feedforward system with the virtual sensing techniques [21], [22] are potential future work directions.

References

[1] Y. Kajikawa, W.-S. Gan and S. M. Kuo, 'Recent advances on active noise control: Open issues and innovative applications', *APSIPA Trans. Signal, Inf. Process.*, vol. 1, 2012, ISSN: 2048-7703.

[2] J. Zhang, T. D. Abhayapala, W. Zhang, P. N. Samarasinghe and S. Jiang, 'Active noise control over space: A wave domain approach', *IEEE/ACM Trans. Audio, Speech, Language Process*, vol. 26, no. 4, pp. 774–786, 2018, ISSN: 2329-9290.

[3] H. Ito, S. Koyama, N. Ueno and H. Saruwatari, 'Feedforward spatial active noise control based on kernel interpolation of sound field', in *ICASSP 2019 - 2019 IEEE International Conference on Acoustics, Speech and Signal Processing (ICASSP)*, 2019, pp. 511–515, ISBN: 2379-190X.

[4] H. Sun, T. D. Abhayapala and P. N. Samarasinghe, 'Active noise control over 3D space with multiple circular arrays', in *2019 IEEE Workshop on Applications of Signal Processing to Audio and Acoustics (WASPAA)*, 2019, pp. 135–139, ISBN: 1931-1168.

[5] Y. Maeno, Y. Mitsufuji, P. N. Samarasinghe, N. Murata and T. D. Abhayapala, 'Spherical-harmonic-domain feedforward active noise control using sparse decomposition of reference signals from distributed sensor arrays', *IEEE/ACM Trans. Audio, Speech, Language Process.*, vol. 28, pp. 656–670, 2020, ISSN: 2329-9304.

[6] S. Koyama, J. Brunnstrom, H. Ito, N. Ueno and H. Saruwatari, 'Spatial active noise control based on kernel interpolation of sound field', *IEEE/ACM Trans. Audio, Speech, Language Process.*, pp. 1–1, 2021, ISSN: 2329-9304.

[7] S. M. Kuo and D. Morgan, *Active noise control systems: algorithms and DSP implementations*. John Wiley & Sons, Inc., 1995.

[8] J. A. Zhang, N. Murata, Y. Maeno, P. N. Samarasinghe, T. D. Abhayapala and Y. Mitsufuji, 'Coherence-based performance analysis on noise reduction in multichannel active noise control systems', *J. Acoust. Soc. Am.*, vol. 148, no. 3, pp. 1519–1528, 2020.

[9] H. Chen, P. Samarasinghe, T. D. Abhayapala and W. Zhang, 'Spatial noise cancellation inside cars: Performance analysis and experimental results', in *2015 IEEE Workshop on Applications of Signal Processing to Audio and Acoustics (WASPAA)*, 2015, pp. 1–5.

[10] H. Chen, P. Samarasinghe and T. D. Abhayapala, 'In-car noise field analysis and multi-zone noise cancellation quality estimation', in *2015 Asia-Pacific Signal and Information Processing Association Annual Summit and Conference (APSIPA)*, IEEE, 2015, pp. 773–778, ISBN: 9881476801.

[11] J. Zhang, T. D. Abhayapala, W. Zhang and P. N. Samarasinghe, 'Active noise control over space: A subspace method for performance analysis', *Appl. Sci*, vol. 9, no. 6, p. 1250, 2019, ISSN: 2076-3417.

[12] J. Zhang, H. Sun, P. N. Samarasinghe and T. D. Abhayapala, 'Active noise control over multiple regions: Performance analysis', in *ICASSP 2020 - 2020 IEEE International Conference on Acoustics, Speech and Signal Processing (ICASSP)*, 2020, pp. 8409–8413, ISBN: 2379-190X.

[13] E. G. Williams, *Fourier acoustics: sound radiation and nearfield acoustical holography*. Elsevier, 1999, ISBN: 0080506909.

[14] R. A. Kennedy, P. Sadeghi, T. D. Abhayapala and H. M. Jones, 'Intrinsic limits of dimensionality and richness in random multipath fields', *IEEE Transactions on Signal Processing*, vol. 55, no. 6, pp. 2542–2556, 2007, ISSN: 1053-587X.

[15] H. Chen, J. Zhang, P. N. Samarasinghe and T. D. Abhayapala, 'Evaluation of spatial active noise cancellation performance using spherical harmonic analysis', in *2016 IEEE International Workshop on Acoustic Signal Enhancement (IWAENC)*, 2016, pp. 1–5.

[16] J. B. Allen and D. A. Berkley, 'Image method for efficiently simulating small-room acoustics', *J. Acoust. Soc. Am.*, vol. 65, no. 4, pp. 943–950, 1979. eprint: https://doi.org/10.1121/1.382599.

[17] *RIR generator*, https://www.audiolabs-erlangen.de/fau/professor/habets/software/rir-generator, Accessed: 2019-07-10.

[18] T. Kosaka, S. J. Elliott and C. C. Boucher, 'A novel frequency domain filtered-x lms algorithm for active noise reduction', in *1997 IEEE International Conference on Acoustics, Speech, and Signal Processing*, vol. 1, 1997, 403–406 vol.1, ISBN: 1520-6149.

[19] J. Zhang, W. Zhang and T. D. Abhayapala, 'Noise cancellation over spatial regions using adaptive wave domain processing', in *2015 IEEE Workshop on Applications of Signal Processing to Audio and Acoustics (WASPAA)*, 2015, pp. 1–5.

[20] X. Kong and S. M. Kuo, 'Study of causality constraint on feedforward active noise control systems', *IEEE Transactions on Circuits and Systems II: Analog and Digital Signal Processing*, vol. 46, no. 2, pp. 183–186, 1999.

[21] S. J. Elliott, W. Jung and J. Cheer, 'Causality and robustness in the remote sensing of acoustic pressure, with application to local active sound control', in *ICASSP 2019 - 2019 IEEE International Conference on Acoustics, Speech and Signal Processing (ICASSP)*, pp. 8484–8488, ISBN: 2379-190X.

[22] H. Sun, J. Zhang, T. D. Abhayapala and P. N. Samarasinghe, 'Active noise control over 3d space with remote microphone technique in the wave domain', in *2021 IEEE Workshop on Applications of Signal Processing to Audio and Acoustics (WASPAA)*, pp. 301–305, ISBN: 1947-1629.

APPENDIX

Appendix A. Proof of Theorem 1

The first terms of (15) can be written as

$$E\{\boldsymbol{y}^H\boldsymbol{y}\} = \sum_{i=1}^{D} E\{y_i y_i^*\} + \sum_{i=D+1}^{(2M+1)} E\{y_i y_i^*\}. \qquad (18)$$

Since $\boldsymbol{\Sigma}$ is a rectangular diagonal matrix with D non-zero diagonal elements σ_i, $i = 1, \ldots, D$, the second term of (15) can be written as

$$\begin{aligned} E\{\boldsymbol{y}^H\boldsymbol{\Sigma}\tilde{\boldsymbol{W}}\boldsymbol{\chi}\} &= E\left\{\sum_{i=1}^{D}\sum_{n=1}^{N} y_i^*\sigma_i\tilde{w}_{in}\chi_n\right\} \\ &= \sum_{i=1}^{D}\sigma_i\sum_{n=1}^{N}\tilde{w}_{in}E\{y_i^*\chi_n\}, \\ &= \sum_{i=1}^{D}\sigma_i\tilde{\boldsymbol{w}}_i E\{\boldsymbol{\chi}y_i^*\}, \end{aligned} \qquad (19)$$

where $\hat{w}_{in}$ is the (i, n) element of $\tilde{\boldsymbol{W}}$ and $\tilde{\boldsymbol{w}}_i \triangleq [\tilde{w}_{i1}, \cdots, \tilde{w}_{iN}]$ is $1 \times N$ vector.

Similarly, the third term in (15) can be written by

$$E\{\boldsymbol{\chi}^H\tilde{\boldsymbol{W}}^H\boldsymbol{\Sigma}^H\boldsymbol{y}\} = \sum_{i=1}^{D}\sigma_i^* E\{y_i\boldsymbol{\chi}^H\}\tilde{\boldsymbol{w}}_i^H. \qquad (20)$$

The fourth term in (15) can be expressed as

$$\begin{aligned} E\{\boldsymbol{\chi}^H\tilde{\boldsymbol{W}}^H\boldsymbol{\Sigma}^H\boldsymbol{\Sigma}\tilde{\boldsymbol{W}}\boldsymbol{\chi}\} &= E\left\{\sum_{i=1}^{D}\sum_{n=1}^{N}\sum_{n'=1}^{N}\chi_n^*\chi_{n'}\tilde{w}_{in}^*\tilde{w}_{in'}\sigma_i^*\sigma_i\right\} \\ &= \sum_{i=1}^{D}\sum_{n=1}^{N}\sum_{n'=1}^{N}|\sigma_i|^2\tilde{w}_{in}^*\tilde{w}_{in'}E\{\chi_n^*\chi_{n'}\}. \end{aligned} \qquad (21)$$

From the eigen-decomposition characteristics of (13), we can write, for $n \le N$,

$$E\{\chi_n^*\chi_{n'}\} = \begin{cases}\lambda_n & n = n' \\ 0, & n \neq n'\end{cases}, \qquad (22)$$

where $\lambda_n \neq 0$. Thus, (21) can be rewritten as

$$\begin{aligned} E\{\boldsymbol{\chi}^H\tilde{\boldsymbol{W}}^H\boldsymbol{\Sigma}^H\boldsymbol{\Sigma}\tilde{\boldsymbol{W}}\boldsymbol{\chi}\} &= \sum_{i=1}^{D}|\sigma_i|^2\sum_{n=1}^{N}\tilde{w}_{in}^*\lambda_n\tilde{w}_{in} \\ &= \sum_{i=1}^{D}|\sigma_i|^2\tilde{\boldsymbol{w}}_i\tilde{\boldsymbol{\Lambda}}\tilde{\boldsymbol{w}}_i^H, \end{aligned} \qquad (23)$$

where $\tilde{\boldsymbol{\Lambda}}$ is a $N \times N$ diagonal matrix whose diagonal elements are the non-zero diagonal elements of $\boldsymbol{\Lambda}$.

By substituting (18), (19), (20) and (23) into (15), using the identity for completing squares for vectors, and denoting $S_{\boldsymbol{xy}} = E\{\boldsymbol{x}\boldsymbol{y}^H\}$, we can obtain

$$\begin{aligned} \mathcal{E} =& \sum_{i=1}^{D}\left(S_{y_iy_i} - \boldsymbol{S}_{y_i\boldsymbol{\chi}}\tilde{\boldsymbol{\Lambda}}^{-1}\boldsymbol{S}_{\boldsymbol{\chi}y_i}\right) + \\ & \sum_{i=1}^{D}\left(|\sigma_i|^2(\tilde{\boldsymbol{w}}_i + \frac{\boldsymbol{S}_{y_i\boldsymbol{\chi}}}{\sigma_i}\tilde{\boldsymbol{\Lambda}}^{-1})\tilde{\boldsymbol{\Lambda}}(\tilde{\boldsymbol{w}}_i + \frac{\boldsymbol{S}_{y_i\boldsymbol{\chi}}}{\sigma_i}\tilde{\boldsymbol{\Lambda}}^{-1})^H\right) \\ & + \sum_{i=D+1}^{2M+1} S_{y_iy_i}. \end{aligned} \qquad (24)$$

Equation (24) can be rearranged in the form of (16) in Theorem 1.